An alternative approach to automotive ESC based on measured wheel forces

An alternative approach to automotive ESC based on measured wheel forces

A. Morgando[a], M. Velardocchia[a], A. Vigliani[a]**, B.G. van Leeuwen[b] and V. Ondrak[b]

[a]*Politecnico di Torino, Dipartimento di Meccanica, 10129 Torino, Italy*; [b]*SKF Automotive Division, SKF B.V., 3439 MT Nieuwegein*

Keywords electronic stability control; load sensing bearings; hardware-in-the-loop

Abstract *Traditional electronic stability control (ESC) systems act on one or more wheels on the basis of a logic aiming at the control of variables that cannot be directly measured (vehicle sideslip angle and tire slip). Hence it is necessary a vehicle state estimator capable of evaluating the needed variables from the data of the input sensors. In the present paper the authors discuss a different approach to the estimation problem, assuming that the forces acting on the wheels can be directly measured. ESC feed forward control logic is designed through vehicle frequency response analysis in order to obtain a faster active system activation. The variable controlled by the logic is the wheel longitudinal force. Experimental results obtained on an ESC hardware in the loop (HIL) test bench prove the validity of the approach showing enhanced dynamic performances, together with the limits due to the delays in the actuation of the ESC motor pump, which needs some time to build the pressure requested for intervention on the selected callipers. Finally, the tests demonstrate the opportunity of closing the control loop on a variable (i.e., the force) that can be directly measured.*

**Corresponding author. Email: alessandro.vigliani@polito.it

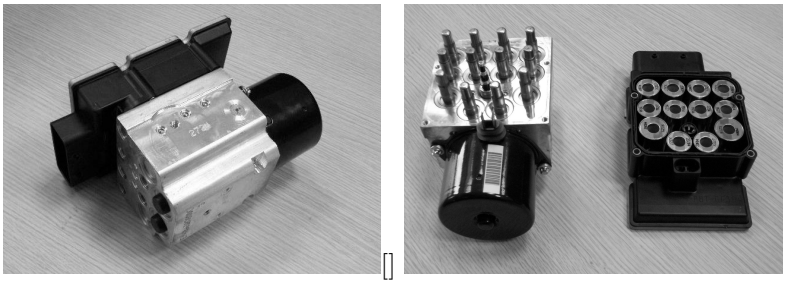

Figure 1: Normal production ESC unit: assembled (a) and after the separation of control and hydraulic unit (b).

1 Introduction

The Electronic Stability Control (ESC) is a vehicle dynamics control system aimed at increasing safety by assisting the driver in controlling the car during cornering manoeuvres. It is also known as Vehicle Dynamics Controller (VDC) or Electronic Stability Program (ESP).

ESC was firstly introduced by Bosch in mass produced cars at the end of the twentieth century and is getting more and more popular in the automotive market. Van Zanten et al. describe the basic concept behind the control logic and actuation systems [[1, 2]]. A commercial ESC unit (Figure 1) consists of an electro-hydraulic unit (HCU) integrated in the former vehicle braking system: it is composed of twelve electro-valves and a motor pump, used to vary the brake pistons pressure independently of the driver action on the brake pedal. The hydraulic unit is activated by an electronic control unit (ECU), shown in Figure 1(b) where the ECU is separated from the hydraulic unit.

The aim of ESC is to reduce the vehicle understeer or oversteer thanks to proper corrective braking and engine torque. Sensors are used to estimate the vehicle conditions, mainly in terms of longitudinal and lateral accelerations, yaw velocity and vertical load. Basically the desired vehicle yaw rate $\dot{\psi}_{ref}$ is computed, according to the driver's input, with the following equation (see [3]):

$$\dot{\psi}_{ref} = \frac{\frac{\delta_w}{R_s} V}{L + \frac{K_u}{g} V^2} \tag{1}$$

where L is the vehicle wheelbase, K_u is the understeer coefficient, δ_w is the steering wheel angle, V is the vehicle speed, R_s is the steering ratio and g is the gravity acceleration.

Further developments of the ESC logic focuses on the vehicle sideslip angle active control, since an uncontrolled increase of its value leads to a loss of vehicle stability even in case of low yaw rate, as demonstrated by Shibahata [4]. Two possible means of dealing with sideslip control are

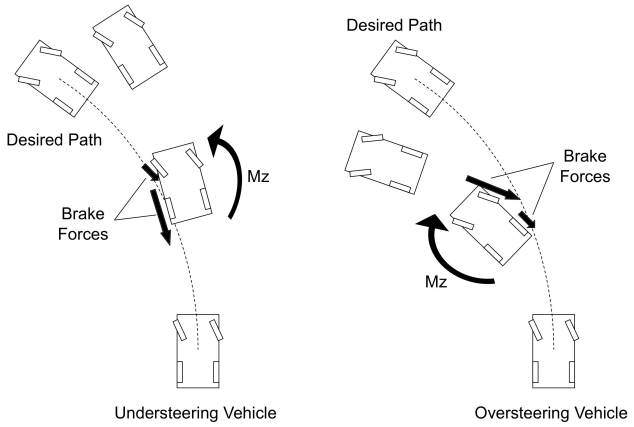

Figure 2: ESC activation comparison in case of oversteer and understeer, in terms of which wheels are braked and which wheel is braked mainly.

- the correction of the reference yaw rate in case of sideslip deviation from the reference value, as suggested in [1];
- the definition of a threshold value under which the sideslip must be kept, as proposed in [5].

A simple control approach is to compare the reference yaw rate and sideslip values with the vehicle actual condition, in order to determine the vehicle oversteer or understeer behaviour.

During cornering, saturation of the tyres lateral force may occur, thus leading to a nonlinear behaviour of the vehicle. The ESC actuation results in an active behaviour that the average driver recognizes more easily as linear [6]. Thus the efficiency of ESC intervention is determined observing yaw rate peak reduction and oscillation damping time during cornering, together with vehicle sideslip angle containment and little longitudinal speed loss due to brakes intervention. As shown in Figure 2 an ESC can generate a yaw moment, which is added to moment M_z generated by the tyre forces during cornering, in order to correct the vehicle dynamics, thereby improving its handling and stability [1].

During cornering, braking the outer wheels generates a moment opposite to yaw, thus reducing the yaw moment generated by the steered wheels, and therefore contrasting possible oversteer. Vice versa, braking the inner wheels provokes a greater total yaw moment, in order to reduce the understeer behaviour. Moreover, in case of understeering the main braking action should occur on the inner rear wheel, because the increase of the tyre longitudinal force due to braking would produce as side effect a reduction of lateral force of the same tyre, thus determining a decrease of the yaw moment of the tyre forces opposed to the ESC action. For the same reason, in case of oversteering the

outer front tyre should be braked more than the rear one, in order to achieve a larger total yaw moment [1, 5, 7].

A large percentage of ESC system modelling is related to the sensors chosen to provide the driver and vehicle dynamic information [8]. The required data are the steering wheel angle, the vehicle yaw rate and lateral acceleration, the tandem master cylinder pressure and the wheels angular velocity. Several ESC are equipped also with a longitudinal acceleration sensor to better identify the vehicle behaviour. At SKF new Load Sensing Hub Bearing Units (Figure 3) are being developed in order to provide vehicle active systems with direct wheelforce data ([9, 10]). In addition to these wheel forces and speeds, data from additional vehicle sensors are available on the vehicle CAN; the same network is used lo link the control logic to the engine control unit.

The literature on ESC control design is wide. J. Yeop et al. [11] use a vehicle mathematical model to conceive a control strategy that integrates ESC and an active driveline management system, aimed at controlling the yaw rate. Shuibo at al. [12] apply a linear quadratic regulator and sliding mode theories to a wheel slip ratio controller and use it to control the vehicle lateral dynamics. Laine and Andreasson [13] treat the vehicle as an over-actuated system and apply the control allocation methodology to design an ESC logic for the brake system and the engine.

An example of direct yaw control (DYC) application of sliding mode control (SMC) can be found in [14]. The yaw moment necessary for correcting vehicle manoeuvring is determined based on sensor outputs and estimated state variables. The adaptive SMC is designed in order to let the vehicle slide on a surface defined by desired yaw angle ψ and yaw rate $\dot{\psi}$ and by desired sideslip angle β and its derivative $\dot{\beta}$, whose values are determined by an observer.

Sliding mode observers can replace the conventional approach to define the oversteer/understeer behaviour of the vehicle. A sliding mode observer, based on a single track vehicle model and using the principle of the equivalent output error, is used to determine if the vehicle is entering a potentially dangerous situation during a transient manoeuvre ([15]).

Finally, according to van Zanten et al. [1], the desired yaw moment is used with equation (2) to compute the value of the braking forces and, consequently, of the tyre lateral forces required by each wheel:

$$\Delta M_z = -\frac{\partial F_y}{\partial \lambda}\Delta\lambda\left(a\cos\frac{\delta_w}{R_s} - b\sin\frac{\delta_w}{R_s}\right) + \frac{\partial F_x}{\partial \lambda}\Delta\lambda\left(a\sin\frac{\delta_w}{R_s} - b\cos\frac{\delta_w}{R_s}\right) \quad (2)$$

where F_x and F_y are the tyre longitudinal and side forces, λ is the tyre longitudinal slip, a and b are the front and rear wheelbases. Given the tyre forces dependence on longitudinal slip, equation (2) is also used to define the slip variation needed to obtain the proper braking force.

Currently an ESC depends on a set of estimation to actuate the electro-valves and motor pump: a hydraulic model of the brake circuit is used to estimate the actual caliper pressure, so that the control unit can increase or reduce the pressure in order to achieve the desired tyre slip. A few dynamic states are

Figure 3: SKF Load Sensing Hub Bearing Unit.

also estimated, like sideslip angle, position of the centre of gravity and the road lateral and longitudinal slope [2, 11]. Yet these estimations are not reliable enough to be employed in every operating condition by the control logic and have to be reset periodically. Furthermore the exploitation of the brake system by the hydraulic unit is affected by delays which in turn affect also the active system: hence the hardware behaves as a filter with respect to possible improvement in the control logic promptness and bandwidth.

Tyre forces measurement can be used to provide inputs to vehicle states estimators, as described in [16]. Several approaches are suggested, like inverse tyre model or direct integration of tyre forces. Each approach is not fully reliable yet, since road friction is unknown and the estimation algorithm must be periodically reset in order to avoid error propagation through integration. Besides the improvement of estimators and observers, tyre force measurement can be used as direct input for an active braking control logic, used to determine whether an activation is necessary or not. Gobbi *et al.* [17] present a prototype of a tyre forces measurement system; in their work, tyre forces are used to compute the sliding surface of SMC based ABS and ESP.

In the present work a conventional DYC is used, based on the definition of the required yaw moment by comparing actual and reference yaw rate, conventionally computed. This paper describes the design process of an ESC control logic that relies on the knowledge of actual tyre-road forces, due to innovative sensors, able to measure the three components of the wheel forces at a rate of 200 Hz, with accuracy about 5% of full scale ([10]). The logic is aimed only at controlling the vehicle through braking, without any intervention on the engine torque. The control logic is tested experimentally through a hardware in the loop (HIL) test bench in order to observe its capability of controlling a real brake system. Finally, in order to take into account the drawbacks of the hardware delays on the system performance, the electro-valves and motor pump actuation logic is also considered.

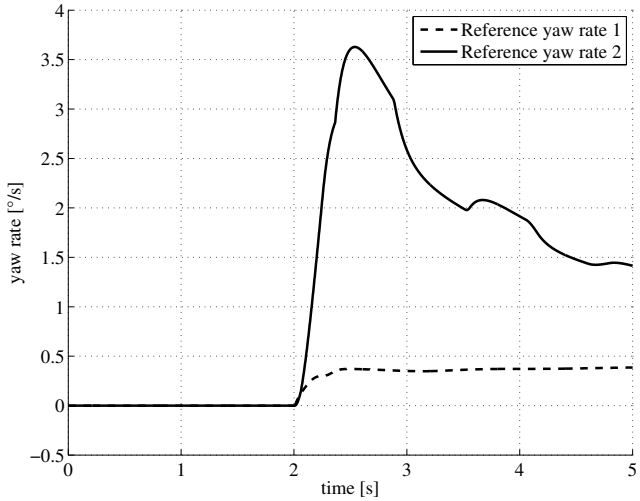

Figure 4: Passive vehicle yaw rate: reference yaw rate obtained with equation (1) and (3) in case of a step steer manoeuvre.

2 ESC logic

The design process starts from a classic closed loop (CL) control strategy. The control signals depend on the difference between the vehicle actual yaw rate and the yaw rate reference value. In order to estimate the reference yaw rate, eq. (1) alone does not give satisfactory results, since in case of large values of the steering wheel angle, the estimated yaw rate would be unreliable. Hence it is necessary to evaluate an alternate estimate of $\dot{\psi}$, i.e.:

$$\dot{\psi}_{ref} = \frac{a_y}{V} \tag{3}$$

where a_y is the lateral acceleration.

The actual value of the reference yaw rate $\dot{\psi}$ is given by the smaller between the values given by eq. (1) and (3) (see Figure 4). Equation (3) allows to evaluate the correct value of the steady state vehicle yaw rate, but its time history does not match the real vehicle's one, since the vehicle lateral acceleration changes more rapidly than the yaw rate during the transient (see Figure 5).

An alternative approach to the definition of the reference yaw rate starts from the characterisation of the vehicle lateral dynamics through a linear mathematical model. A single track vehicle model is built in order to simulate vehicle behaviour in linear conditions, characterised by two degrees of freedom, i.e. lateral velocity and yaw rate. The vehicle longitudinal velocity is considered constant and treated as an internal parameter. Since the application of the linear model concerns the ESC actuation, a second input is considered beside the steering wheel angle, representing a generic yaw moment M_z around the centre

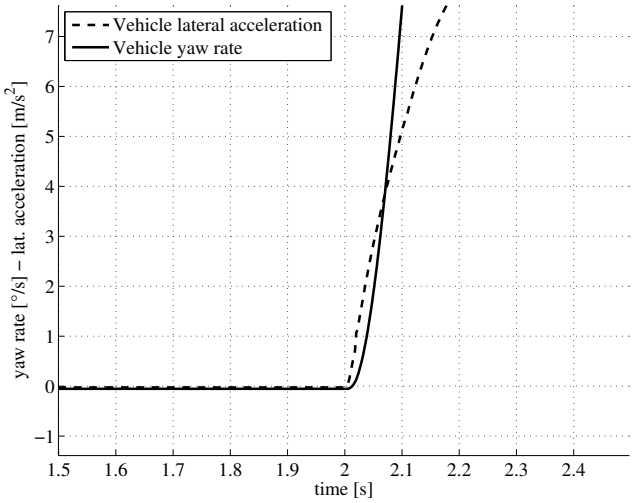

Figure 5: Passive vehicle: yaw rate and lateral acceleration during the transient of a step steer manoeuvre.

of mass. The latter input is used to simulate the action of an active system such as an ESC. Equations (4) describe the system dynamics:

$$\begin{cases} M_z + F_{y,f}a - F_{y,r}b = I_z\ddot{\psi} \\ F_{y,f} + F_{y,r} = mV\left(\dot{\beta} + \dot{\psi}\right) \\ F_{y,f} = C_f\left(\dfrac{\delta_w}{R_s} - \beta - \dfrac{a}{V}\dot{\psi}\right) - \dfrac{k'_f}{V}\dot{F}_{y,f} \\ F_{y,r} = C_r\left(\beta - \dfrac{b}{V}\dot{\psi}\right) - \dfrac{k'_r}{V}\dot{F}_{y,r} \end{cases} \tag{4}$$

where I_z is the vehicle moment of inertia about vertical axis z, m is the sprung mass, β is the sideslip angle, C is tyre cornering stiffness, k' is tyre relaxation length, while subscripts $_f$ and $_r$ respectively refer to front and rear.

The model parameters are set in order to refer to a medium European sedan. The transfer function (5) between the steering wheel angle and the vehicle yaw rate, obtained from the linear model, describes the behaviour of the passive vehicle:

$$\left(\frac{\dot{\psi}}{\delta_w}\right)_P = VC_f\frac{mak'_rs^2 + maVs + aC_r + bC_r}{d_4s^4 + d_3s^3 + d_2s^2 + d_1s + d_0} \tag{5}$$

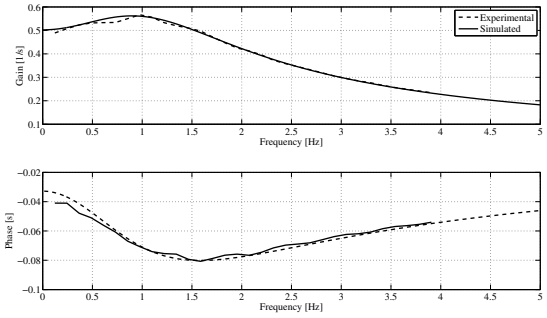

Figure 6: Comparison between experimental and simulated yaw rate frequency responses.

where

$$
\begin{aligned}
d_4 &= mI_z k'_f k'_r \\
d_3 &= mI_z V k'_f + mI_z V k'_r \\
d_2 &= I_z k'_f C_r + ma^2 k'_f C_f + mb^2 k'_f C_r + I_z k'_r C_f + mI_z V^2 \\
d_1 &= I_z V C_r + mb^2 V C_R + mbk'_f V C_r + ma^2 V C_f + I_z V C_f - mak'_r V C_f \\
d_0 &= b^2 C_f C_r - maV^2 C_f + 2abC_f C_r + a^2 C_f C_r + mbV^2 C_r
\end{aligned}
\tag{6}
$$

Transfer function (5) is characterized by two natural frequencies and two damping ratios, while the numerator has two zeros. Thus function (5) can be defined through seven parameters, including the function gain. Figure 6 shows the validation of the linear model, obtained from the comparison of the experimental frequency response of the vehicle and the frequency output of the transfer function. The manoeuvre used to validate the model is usually called "sweep steer manoeuvre" and is based on a sinusoidal motion of the steering wheel, characterised by an amplitude of 20°. The manoeuvre is performed at a longitudinal speed equal to 120 km/h and the frequency of steering wheel motion is gradually increased until reaching 5 Hz. The sweep steer is performed by a test pilot with the real vehicle; then the steering time history is used as input for the vehicle model. A frequency response analysis is performed on the yaw rate time history and the experimental results are compared with the simulation, as shown in Figure 6. The phase in the diagram is expressed in seconds, meaning the time delay between the driver's steering command and the vehicle yaw response; the value is obtained dividing the phase [rad] by the corresponding frequency [rad/s].

In order to adjust the yaw rate reference value to the actual vehicle speed the following equation can be applied:

$$
\dot{\psi}_{ref} = \dot{\psi} \left(\frac{V}{V_{set}} \right) \tag{7}
$$

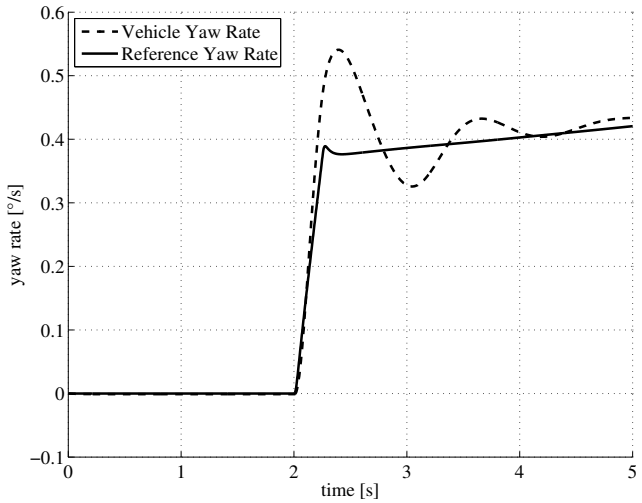

Figure 7: Passive and reference yaw rate obtained through equation (6) for a step steer manoeuvre.

where V_{set} is the value of vehicle longitudinal speed introduced in the linear model as a constant parameter.

After the validation of the linear model, a target transfer function $(\dot{\psi}/\delta_w)_T$ is computed, representing the vehicle desired behaviour after the correction added by the ESC (see Figure 7). The new transfer function defines the reference yaw rate according to the steering wheel input and does not depend on physical parameters but is chosen by the control designer. The aim of the target function can be, e.g., to obtain an active vehicle characterized by an over-damped behaviour. Moreover, to consider the effects of the active control alone on the vehicle yaw rate, transfer function $(\dot{\psi}/M_z)_T$ can be defined. The difference between desired and actual behaviour transfer functions defines a new single input – single output (SISO) control transfer function $(M_z/\delta_w)_C$, as described in equation (8), where $(M_z/M_{z,act})$ is the transfer function describing the non ideal behaviour of the control system actuator:

$$\left(\frac{M_z}{\delta_w}\right)_C = \frac{\left(\frac{\dot{\psi}}{\delta_w}\right)_T - \left(\frac{\dot{\psi}}{\delta_w}\right)_P}{\left(\frac{\dot{\psi}}{M_z}\right)\left(\frac{M_z}{M_{z,act}}\right)} \tag{8}$$

The results presented in this paper are obtained considering an ideal rear actuator, thus $(M_z/M_{z,act}) = 1$. The analysis of the results will show that this assumption is wrong and the influence of the ESC actuator cannot be neglected, but has to be compensated in some way.

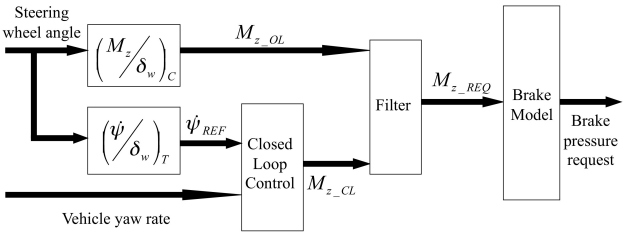

Figure 8: Control logic diagram.

Function $(M_z/\delta_w)_C$ represents the feed forward control logic, which imposes the ESC intervention as a result of the steering wheel motion. The driver's impulsive steering wheel rotation is interpreted as a quick yaw rate request and if necessary the ESC compensates passive vehicle yaw response delay. Transfer function output determines the brakes pressure p_t request by brake system mathematical model:

$$p_t = \frac{2M_z}{t}\frac{R}{\mu E_s B_F} \tag{9}$$

where R is the tyre radius, t is the vehicle track, E_s is the booster coefficient, μ the friction coefficient between disk and pad and B_F is the brake factor.

The logic allows two wheels to be braked at the same time, on the same side of the car. The model recognizes steering wheel rotation direction and vehicle oversteer or understeer condition. ESC is requested to generate the proper yaw moment M_z through front and rear wheels braking. Front and rear brake force split is determined by two complementary coefficients, whose values depend on which wheel is chosen to brake more heavily. Feed-forward (FF) control reaches its limits when tyres saturate and present nonlinear behaviour, depending on road friction. A similar consideration holds in case of low adherence, or considering the temperature and components wear influence on the brake system performance. Thus a control logic based on linear hypothesis alone is not considered safe enough. The transfer function is then merged in a closed loop control structure in order to ensure failsafe conditions and control robustness. Yaw reference value calculation method is modified for the closed loop: it is now defined by the transfer function $(\dot{\psi}/\delta_w)_T$. Closed loop (CL) controller parameters are set in order to let CL only adjust the control signal coming from open loop (OL) transfer function. Final control logic structure is represented in Figure 8. FF and CL work independently; then their contributions are summed and processed through a filter dependent on derivative value. The filter aim is to avoid ESC prolonged intervention or improper activation in case of little differences between vehicle yaw rate reference and actual values. Theoretically, if compared to a closed loop control alone, a feed forward grants a quicker intervention.

3 Control logic based on Load Sensing Hub Bearing Unit

The former logic can be improved in case innovative sensors able to measure the forces at the wheels are available. A possible advantage given by the measure of the ground forces lies in the chance of directly controlling the forces exerted by the wheels, without need of a model to estimate the brake pressure or the tyre longitudinal slip. The control transfer function output can be obtained by tyre braking forces, as defined by the following equations:

$$\begin{cases} M_{z,l} = -F_x \left(\dfrac{t}{2} \cos \delta_f - a \sin \delta_f + k_p \dfrac{t}{2} \right) \\ M_{z,r} = F_x \left(\dfrac{t}{2} \cos \delta_f + a \sin \delta_f + k_p \dfrac{t}{2} \right) \end{cases} \tag{10}$$

where $\delta_f = \delta_w / R_s$ is the front steering angle.

The first of eq.(10) is valid if the yaw moment is obtained by braking the left (subscript $_l$) tyres, while the second holds if the right (subscript $_r$) tyres are braked. In both cases, the rear wheel braking force is dependent on the front one according to a proportional coefficient k_p, whose value varies between 0 and 1. In this way, e.g. in case of oversteering, the front wheel is braked more than the rear and vice-versa, as expressed by equations:

$$\begin{cases} T_{r,o} = k_p T_f & \text{(oversteer)} \\ T_{r,u} = (1 - k_p) T_f & \text{(understeer)} \end{cases} \tag{11}$$

After the definition of the reference braking force, the actuation logic is changed in order to realize a force control. The desired force is compared with the actual braking force computed from the sensor signal. The braking cylinder pressure is increased or reduced in order to minimize the difference between these two values, thus defining two distinct states in which the active system can operate. Since the brake pressure gradient during the increase and reduction phases is high, the pressure is never kept constant; hence the pressure maintenance phase is not included in the final control logic. A dead zone limited at 100 N is applied for the control error, to avoid undesired actuation.

4 Simulation results

Simulation results are obtained on a 14 degrees of freedom vehicle model: six for the car body, one for each wheel rotation and vertical travel; suspensions characteristics are included. The model includes a hydraulic brake system model, obtained through several tests performed using the test bench described in the following section. The model is validated using road test data of a front driven sedan (see Tab. 4 for the main vehicle data), characterized by design parameters equal to those of single track model. The manoeuvre chosen to test the algorithm is a classical step steer, characterized by the vehicle running at 100 km/h

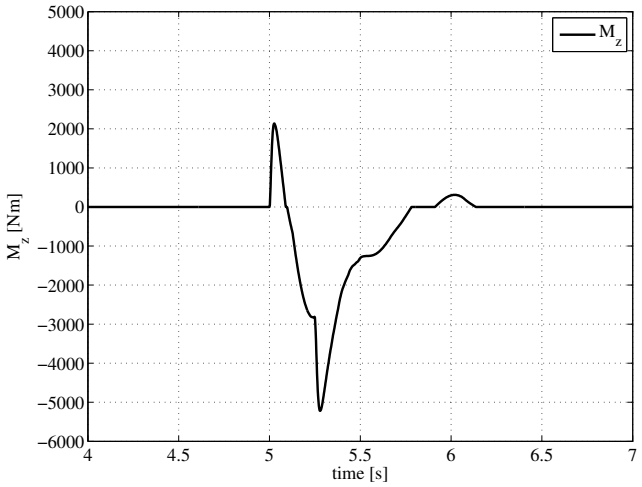

Figure 9: Yaw moment requested by the open loop control logic during a step steep manoeuvre.

and undergoing a sudden steer of 100° with a 400°/s wheel angle rate, which is considered a highly nonlinear manoeuvre. The manoeuvre is performed during a throttle pedal release, in order to minimize the influence of the driving torque and consequently the lack of a traction control logic running together with the brake pressure control. Figure 10 shows the value of the requested yaw torque determined by the open loop control.

Table 1: Main data of the vehicle used in tests

mass m	1580	kg	inertia I_z	$2.21 \cdot 10^3$	kg m^2
track t	1.59	m	steering ratio R_s	13.1	-
front wheelbase a	0.977	m	rear wheelbase b	1.723	m
front spring k_f	$43{\cdot}10^3$	N/m^2	rear spring k_r	$27{\cdot}10^3$	N/m
front damper c_f	$2.6{\cdot}10^3$	Ns/m^2	rear damper c_r	$2.1{\cdot}10^3$	Ns/m
tyres	225/50 R 17	-			

The active control is composed by three phases. Considering that steering action begins at 5 s and that in the first tenth of second the yaw reference is greater than passive yaw (see Figure 9), the control logic immediately requests a yaw moment increase in order to obtain a quicker cornering. The second request is for a counter-yaw moment to reduce the positive peak value of yaw rate, which characterizes the passive vehicle after 0.5 s from the beginning of the manoeuvre. The third phase of the ESC activation is a yaw moment request

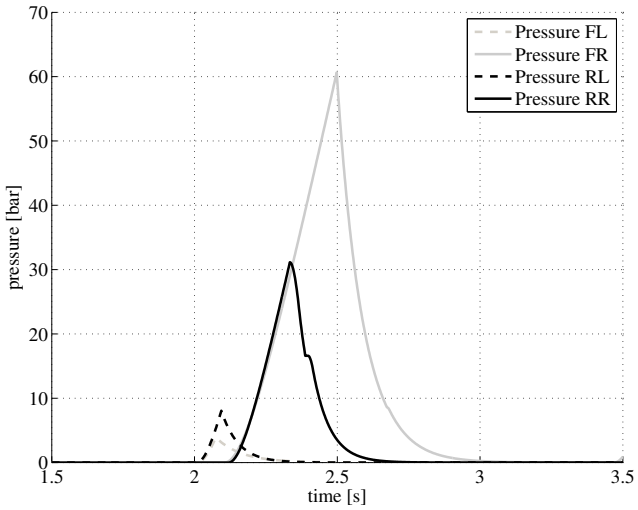

Figure 10: Brake pressure obtained from the open loop yaw moment request.

aimed at damping the yaw rate residual oscillations. Figure 9 shows the values of the simulated brake cylinder pressures derived from the active torque request, setting $k_p = 0.5$.

Considering the pressure at the main braked wheel (Figure 10), the first phase of the control is turned into a pressure of 5 bar, the second phase reaches 30 bar, while the third phase is absent. Due to the proportionality between yaw moment and pressure in eq. (9), the pressure for the first phase should be at least three times higher, but the delay due to the motor pump does not allow the pressure to reach the desired value so promptly. For the same reason the third phase of the activation is filtered. Results show that the hydraulic unit has a great influence on the potential exploitation of the active system; for this reason it is necessary to proceed to hardware experimentation.

5 HIL test rig experimentation

5.1 Test bench

Test experimentation is based on the use of a hardware in the loop (HIL) test bench. The test rig is adapted in order to mount the original components of the brake system of the vehicle used to validate the mathematical model (Figure 11). It consists of the entire brake system, comprehensive of vacuum booster, tandem master cylinder (TMC), electronic stability control unit, all rigid and flexible pipes mounted on the real car and four wheel discs with brake callipers. A controlled actuator pushes the booster input rod, allowing to simulate both semi-stationary and dynamic brake manoeuvres. A displacement sensor is mounted

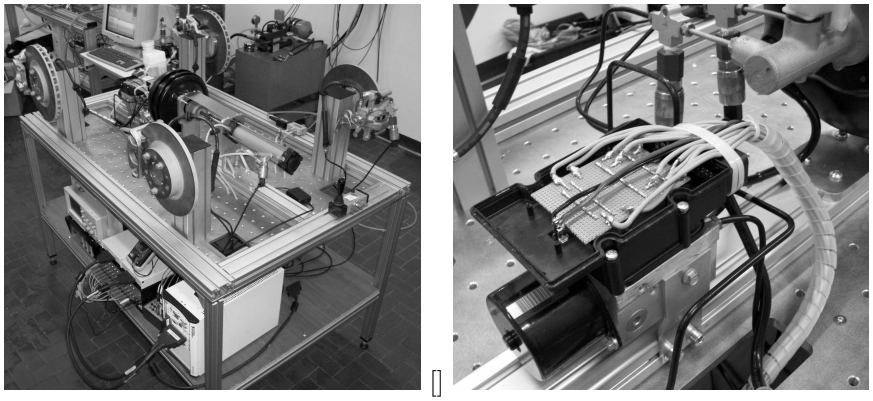

Figure 11: Hardware in the loop test bench (a) for braking system with ESC unit (b) modified in order to bypass the commercial control logic.

on the actuator to measure the feedback of the PID controller, which can work as displacement, speed or pressure controller. Vacuum levels are measured and maintained constant inside the booster. Dedicated sensors measure the pressure at wheel brake cylinders and at TMC. The vehicle model described above runs in real time on a dedicated platform, equipped with data acquisition and signal generation boards.

The original ECU and power electronics are bypassed. The solenoids devoted to the actuation of the 12 electro-valves lay under the circuit of the ECU and the relays are used to activate the motor pump. The circuit is removed and substituted with a plate containing only the welding spots to the solenoid pins. The plate in Figure 11 shows the connections with the electro-valves (12 for the positive pole and 1 for common ground) and a couple of cables devoted to transmit the power signal to the motor pump. Since the real time platform signals need to be turned into power signals, a dedicated box, equipped with high performance solid-state relays, substitutes the motor and valves relays. In order to identify the model parameters for the brake system and to design the ESC control algorithms, it is necessary to identify the main characteristics of the hardware components of the brake system and to test the performances of the passive system. It is also necessary to measure the geometric characteristics of the components of the brake system and of the ESC hydraulic unit: front and rear disc diameters, pad diameters, brake cylinder diameters, pump displacement, high and low pressure accumulator characteristics. Then it is necessary to determine the dynamic characteristics of TMC, valves and motor pump.

5.2 Test procedure to identify electro-valves dynamics

Figure 12 plots a typical test of the brake system dynamics. The brake pedal motion is realised, but the isolation valves are closed in order to maintain the

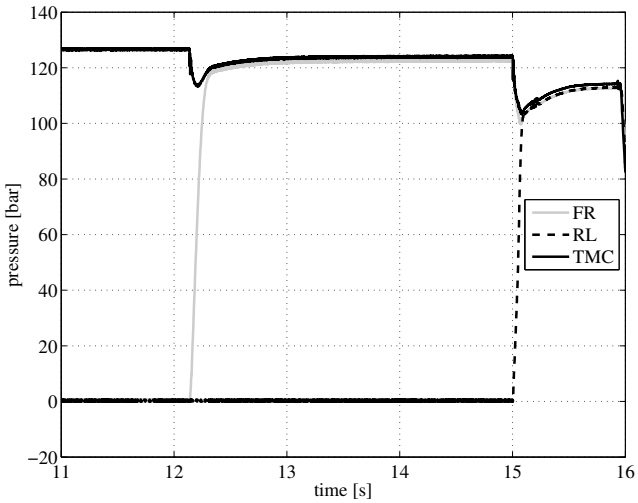

Figure 12: TMC and brakes pressures time history during an electro-valves characterization test.

calliper pressure to zero during the TMC pressure increase. After the TMC pressure reaches the desired value, one ore more isolation valves are opened at the same time, letting the brake fluid to flow to the callipers. The consequent pressure increase is measured, in order to get the average time delay of the brake system. Figure 12 also shows that the isolation valve opening provokes a temporary reduction of the pressure at the TMC: the phenomenon also occurs at the brake calliper piped on the same diagonal. Another test consists in the activation of the motor pump and the proper electro-valves, in order to generate a pressure build-up even when the brake pedal is not pressed. Again the pressure increase is measured and the time vs. pressure characteristic of the motor pump is obtained, as shown in Figure 13. The high frequency oscillation of the pressure, which is superimposed to the build-up curve, is due to the double effect piston motor-pump. The experimental results of the tests carried on ESC valves, motor pump unit and booster allow to describe the dynamics behaviour of the entire brake system with suitable transfer functions. The results are processed in order to set the parameters of the mathematical model of the braking system used in Section 4. It is of interest noting that the mathematical model of the actuator is characterized by a transfer function that reproduces the time delay of the electro-valves but neglects the disturbance during their commutation. Moreover, the motor pump is modelled through a look-up table, neglecting the pressure oscillations.

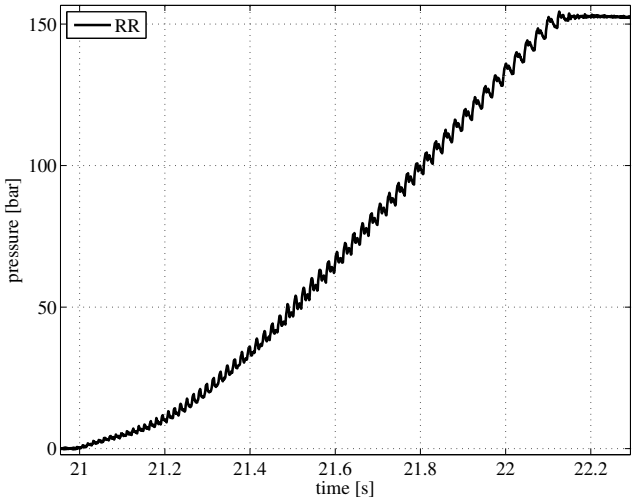

Figure 13: Brake pressure time history during a motor pump characterization test.

5.3 Results

The simulated manoeuvre is described in section 4. The coefficient k_p is set equal to 1 in order to observe the effect of the braking of a single wheel. Further work will focus on the sensitivity of the ESC performance to k_p. Figures 14 and 15 plot a comparison, in terms of body sideslip angle and yaw rate, of the passive vehicle and the active model with open and closed loop algorithms. It is interesting to observe that the two logics give approximately the same results, improving the passive vehicle behaviour thanks to reduced peak values of the oscillations of sideslip angle and yaw rate; moreover also the settling time appears reduced. The small difference between the two active vehicles is due to the not ideal HCU: in fact, the positive peak of sideslip angle at beginning of the manoeuvre is not reduced because of the delay in the pressure build-up during the first phase of ESC activation. The yaw acceleration does not change in the first tenth of second as well, regardless of the yaw moment request by the control logic feed forward.

Figure 16 plots the comparison between requested and obtained tyre longitudinal forces: while the force is well controlled during the reduction phase, the control shows great delay in case of a force increasing request. From the tests it appears that the feed forward action, which should improve the system promptness, has a limited effect due to the delays in the actuation of the ESC motor pump, which needs some time to build the pressure requested for an effective intervention on the selected calliper. The ESC activation is performed on each of the four wheels, instead of only two as stated in Section 2, because the closed loop control adds the chance of braking the outer-rear and

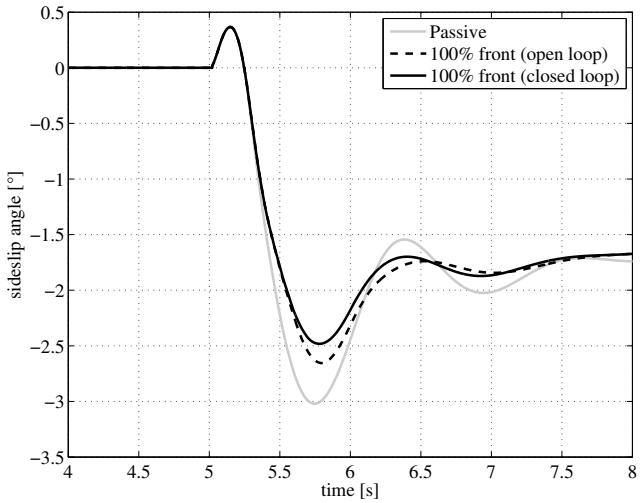

Figure 14: Sideslip angle time history: comparison between passive vehicle, vehicle with open loop ESC and closed loop ESC during a step steer manoeuvre.

the inner-front wheels as well. The tyre longitudinal force can be controlled once it has reached the reference value. It demonstrates the opportunity of closing the control loop on a variable that can be directly measured. Figure 17(a) shows the brake cylinder pressures obtained by the actuation logic in case of a open loop control: the moment request is achieved by braking only two wheels. Figure 17(b) is similar but is obtained through the closed loop control: the difference are small and consequently they have almost the same effect on the vehicle dynamics. Nevertheless, for the selected manoeuvre the closed loop strategy succeeds in giving better results, thanks to the high controllability of the braking forces and the distribution of the activation on four wheels, thus emphasising the greatest advantage of a force based control. Moreover Figure 18 plots the time history of the activation signals for the ESC electro-valves (ISO, DUMP, TC-ISO and TC-SUPPLY) that permit to obtain the desired pressure build-up shown in Figure 17(a).

6 Conclusions

The approach proposed in the paper leads to the design of a true closed loop control strategy, which can be easily tuned. Seven parameters are needed to define the passive vehicle behaviour, seven for the desired active behaviour and one to tune the braking force distribution between front and rear wheels. The main advantage of the approach is that the active system is no more dependent on state observer, since the controlled variable is directly measured. Estimation algorithms, such as brake pressure estimation, which is inevitably affected by

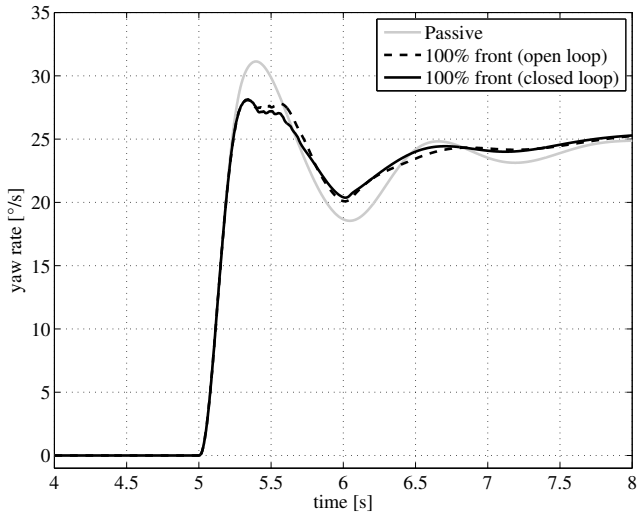

Figure 15: Yaw rate time history: comparison between passive vehicle, vehicle with open loop ESC and closed loop ESC during a step steer manoeuvre.

errors due to nonlinearities, temperature variations and brake component wear, are overcome. Problems have been encountered during the control logic experimentation, since the hydraulic unit response to command signals is affected by several delays, particularly during the early phase of the activation. Such not ideality can be overcome only by changing the hardware design. Future development will concern the simulation of different dynamic manoeuvres, in order to test the logic in a wider range of road conditions and driver's commands. Moreover the control logic will be developed in order to consider lateral and vertical forces measurements, hence to adapt the yaw moment request to load transfer and to tyre lateral saturation.

References

[1] Van Zanten A.T., Erhardt R., Pfaff G., *VDC, the vehicle dynamics control system of Bosch*, SAE Technical paper 950759, 1995

[2] Van Zanten A.T., *Bosch ESP systems: 5 years of experience*, SAE Transactions, 109 (7), 2000

[3] Pacejka H.B., *Tyre and vehicle dynamics*, Butterworth, Oxford, 2002

[4] Shibahata Y., Shimada K., Tomani T., *Improvement of vehicle maneuverability by direct yaw moment control*, Vehicle System Dynamics, 22, 1993, pp. 465–481

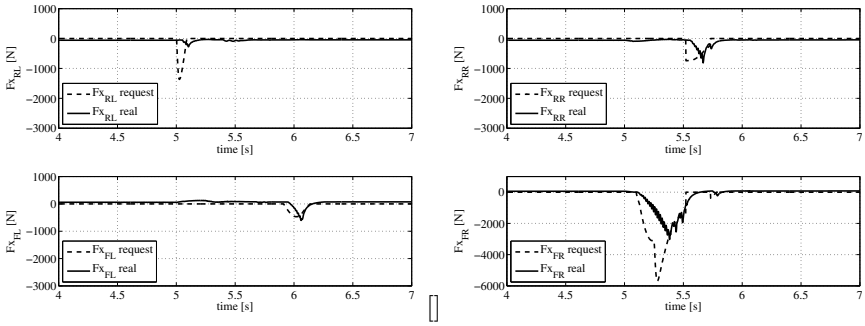

Figure 16: Comparison between requested and actual longitudinal forces for the left (a) and right (b) wheels during a step steer manoeuvre in case of open loop ESC actuation.

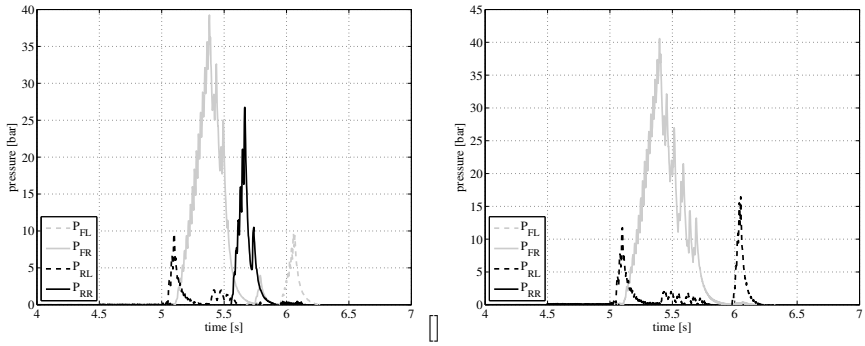

Figure 17: Brake pressure generated by the open (a) and closed (b) loop ESC actuation during a step steer manoeuvre.

[5] Chih-Keng C., Trung-Kien D., Min Fang L., *A compensated yaw moment based vehicle stability controller*, CCDC Proceedings, 2008

[6] Morgando A., *Linear approach to ESP control logic design,* SAE Transactions 115, n.7, 2007

[7] Van Zanten A.T., Erhardt R., Landesfeind K., Pfaff G., *VDC systems development and perspective*, SAE Techinal Paper 980235, 1998

[8] Babala M., Kempen G., Zatyko P., *Trade-offs for vehicle stability control sensor sets*, SAE Technical paper 2002-01-1587, 2002

[9] Mol H. A., *Method and sensor arrangement for load measurement on rolling element bearing based on model deformation*, patent no. PCT/NL2004/000641

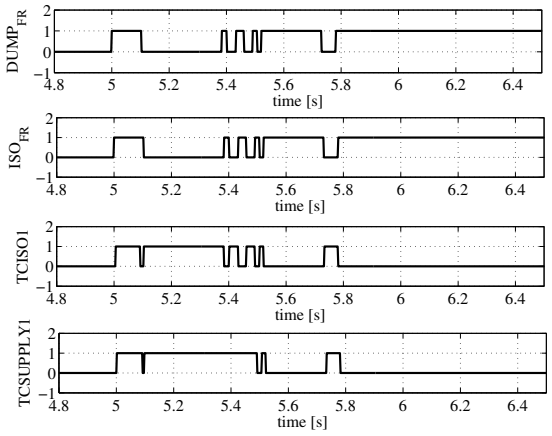

Figure 18: Example of control signals generated by the control logic to the electro-valves of the front right wheel during a step steer manoeuvre in case of open loop ESC actuation.

[10] Zuurbier J., van Leeuwen B., *Vehicle dynamics control based on force-sensing wheel bearings*, Vehicle Dynamics Expo 2007, Messe Stuttgart, Germany, 8-10 May 2007

[11] Jeong Yeop H., Hyeongcheol L., Ji Hwan K., Jeong-Hun K., Byung Hak K., *Coordinated control of the brake control system and the driveline control system*, ICCAS Proceedings, 2007

[12] Shuibo Z., Houjun T., Zhengzhi H., Yong Z., *Controller design for vehicle enhancement*, Control Engineering Practice , 14, 2006, pp.1413–1421

[13] Laine L., Andreasson J., *Control allocation based electronic stability control system for a conventional road vehicle*, ITS Conference, 2007

[14] Yoshioka T., Adachi T., Butsuen T., Okazaki H., Mochizuki H., *Application of sliding-mode theory to direct yaw-moment control*, JSAE Review, 20, 1999, pp. 525–529

[15] Edwards C., Hebden R.G., Spurgeon S.K., *Sliding mode observers for vehicle mode detection*, Vehicle System Dynamics, 43 (11), 2005, pp. 823–843

[16] Krantz W., Neubeck J., Wiedemann J., *Estimation of side slip angle using measured tire forces*, SAE Technical Paper 2002-01-0969, 2002

[17] Gobbi M., Botero J.C., Mastinu G., *Improving the active safety of road vehicles by sensing forces and moments at the wheels*, Vehicle System Dynamics, 46, Suppl., 2008, pp. 957–968